Available online at www.sciencedirect.com

SCIENCE DIRECT®

Advanced Drug Delivery Reviews 57 (2005) 17–42

Advanced DRUG DELIVERY Reviews

www.elsevier.com/locate/addr

Fluorescence techniques for drug delivery research: theory and practice

Nick S. White[a,*], Rachel J. Errington[b]

[a]*Sir William Dunn School of Pathology, University of Oxford, South Parks Road, Oxford, OX1 3RE, UK*
[b]*Department of Medical Biochemistry and Immunology, University of Wales College of Medicine, Cardiff, CF14 4XN, UK*

Received 21 May 2004; accepted 5 August 2004
Available online 27 September 2004

Abstract

Advances in drug delivery require an understanding of drug design, drug stability and metabolism together with the complexities imposed by the biological system such as cell/tissue penetration, drug-target interaction, and the pharmacodynamic consequences. Fluorescence microscopy provides a comprehensive tool for investigating many of these aspects of drug delivery in single cells and whole tissue. This review presents the fundamental concepts of fluorescence-based methodologies. The core principles which underlie the fluorescence process and the interpretation of these events drives instrument design and the components required to illuminate and detect fluorescent probes. Many drugs are inherently auto-fluorescent and therefore can be tracked using microscopy techniques, while other more indirect approaches assay the consequences of drug perturbation. This review addresses the two principle aims in fluorescence microscopy; to generate and enhance fluorescence-derived contrast that may reveal a central process of drug delivery.

Keywords: Fluorescence probes; Fluorescence detection; Fluorescence imaging; Fluorescence microscopy; CCD camera imaging; Laser scanning microscopy; Confocal; Multi-photon; Image restoration; Deconvolution; PSF engineering

Contents

* Corresponding author. Tel.: +44 1865 85740; fax: +44 1865 75515.
E-mail address: nick.white@path.ox.ac.uk (N.S. White).

0169-409X/$ - see front matter © 2004 Elsevier B.V. All rights reserved.
doi:10.1016/j.addr.2004.08.003

1. Introduction

Many biological investigations, and some clinical applications, use the physical properties of electromagnetic radiation in the wavelength range of 190–1100 nm. This covers UV, through to near infrared (NIR) regions of the optical spectrum and it is useful to ask why this range, and the visible portion (400–800 nm) in particular, is widely used for microscopy. Visible light interacts with photoreceptors in our eyes to produce a response. The energy of visible photons is in an appropriate range to be absorbed within living tissues of the eye without damage but specialised molecules must be employed for efficient detection. Evolution has capitalised on this window of opportunity and only very recently have laboratory techniques routinely outperformed natural vision. Biological microscopy is concerned with the shining of light onto cells or tissues, and useful results are obtained when the resultant interactions are significant enough to produce detectable changes in the light. We can turn these changes into image contrast. Two principle aims in microscopy are (i) to generate and (ii) to enhance this contrast for images and measurements.

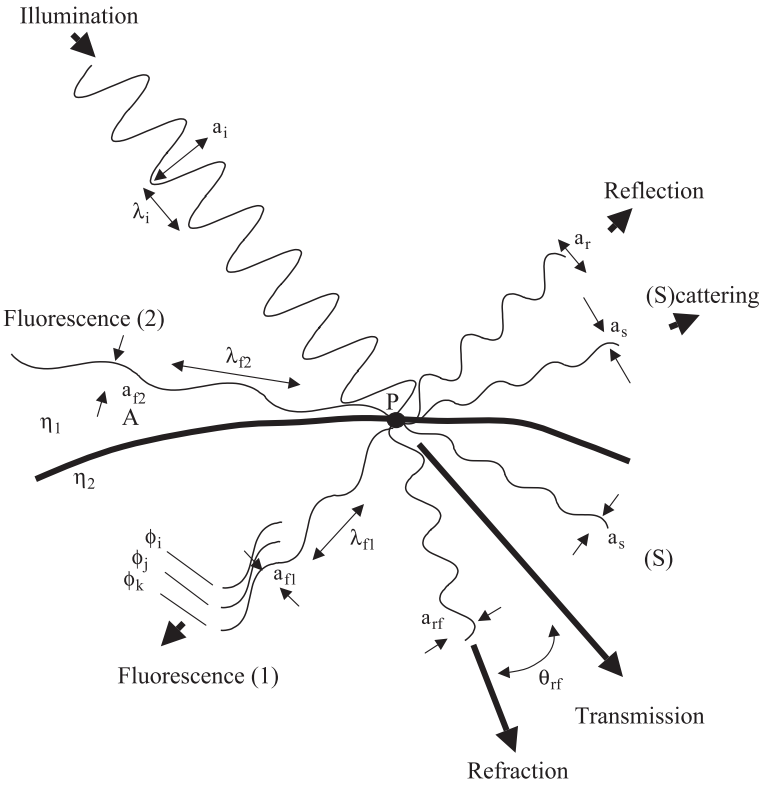

Fig. 1. Diagrammatic representation of some important interactions of light with a specimen. Light of amplitude a_i and wavelength λ_i impinges on a point P at the boundary of two refractive index materials (η_1 and η_2). Light is scattered in all directions with the same wavelength but lower amplitude (a_s) or refracted through an angle θ_{rf} (given by Snell's Law) with amplitude a_{rf}. Fluorescence may occur, depending on chemical components at P, in all directions, with a range of wavelengths and amplitudes (λ_{f1}, λ_{f2}, ... and a_{f1}, a_{f2}, ...). The fluorescence wavefront at any point shows a range of phases (ϕ_i, ϕ_j, ϕ_k, etc) depending on the molecular mobility and the energy level transitions of molecules at P. Absorbance is the ratio of incident light to emitted light.

1.1. Contrast in the optical microscope

Contrast can be described as the ratio of what we wish to observe vs. what we don't, i.e. for an ideal fluorescence instrument:

$$contrast \propto \frac{s}{b+n} \quad \text{where} \quad n \propto \sqrt{(s+b)} \tag{1}$$

and s=average useful signal level (i.e. from biological feature(s) of interest); b=average background (i.e. from uninteresting features); n=noise (statistical variations in s and b).

Several fundamental results follow from this: Firstly, even with no instrument noise, or any background, there is always noise in the signal. Secondly, noise (and also s/n ratio) increases with the square root of signal and background. Finally, it can be just as important to reduce background as it is to optimise signal.

1.2. Contrast modes of the light microscope

Non-fluorescence contrast modes arise from variations of phase, absorbance, scattering, interference, reflection, refraction and/or dispersion of light by the sample (Fig. 1) [1]. These effects are direct consequences of variations in refractive index and mass density, are generally small in unstained biological material and ingenious techniques have been developed to enhance what little contrast is achieved. One such technique is phase contrast microscopy in which phase variations are amplified optically and converted to intensity contrast by annular illumination and a co-aligned 'phase ring' within the objective [2]. Nomarski differential in-

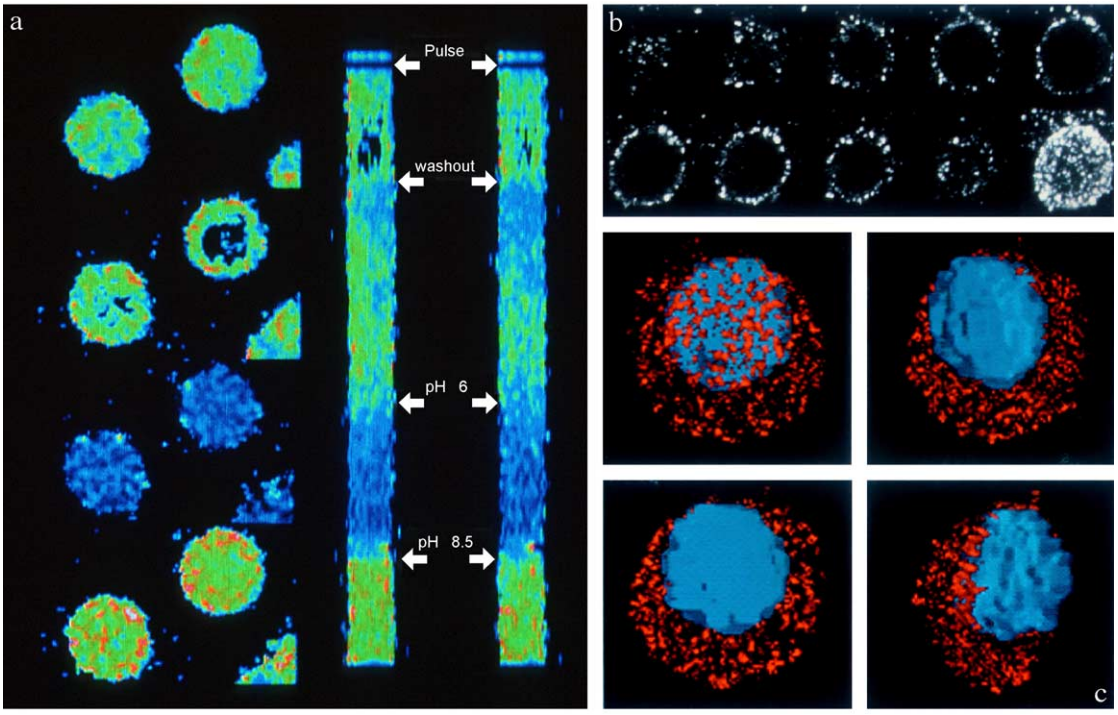

Fig. 2. Multi-dimensional confocal laser scanning fluorescence microscopy of Na^+/K^+ ATPase activity in living chondrocytes. pH fluorescence ratio imaging of live cells using BCECF dye (a). Arrows show (from top) NH_4Cl pulse (alkali load), washout (acid load), pH 6.0 calibration (dark blue) and pH 8.0 calibration (yellow/red). Right hand strips show a single line through each cell followed over time. Ten high resolution optical sections of fluorescence immunostaining of Na^+/K^+ ATPase in a single fixed cell (b). End insert is a digital ensemble of sections. 3-D digital reconstruction of optical sections (c) to show rotated views of ion pump (red) and DNA (blue). Visualising membrane pump activities is key to the study of drug resistance and the regulation of pumps that effect drug uptake into cells. Experimental detail as Mobasheri et al. [67]. Image courtesy of R.J. Errington and A. Mobasheri.

terference (DIC) is an alternative technique in which refractive index gradients impart phase differences (between two cross-polarised beams) that are enhanced using a birefringent element. On recombination of the beams, polarisation is converted to intensity contrast by an 'analyser' [3]. Less commonly used optical methods (e.g. Hoffman modulation) use oblique illumination and/or spatial filters to provide contrast from phase gradients [4]. Light scattering/reflection can also be exploited to provide contrast in biological microscopy in 'dark-field' mode where oblique illumination and blockage of transmitted light are used to detect 'scattered' light [5] or in 'reflection' mode where epi-scopic optics collect reflected light which is distinguished from diffuse 'back scatter' by crossed polarisers [6]. Light scattering or reflection techniques produce contrast against a dark background (e.g. Fig. 2).

1.3. Contrast enhancement using photochemical probes

All of the above contrast methods have shortcomings: (i) they lack chemical specificity (i.e. vary only slowly with the electronic configuration of molecules), and therefore exhibit broad non-specific spectra. (ii) They cannot be easily used to dissect functional aspects of biological systems. (iii) Signal-to-background contrast is often low.

We can overcome these using specific photochemical probes with suitable characteristics in two key components: (i) A 'ligand' component or function—for targeting to the feature or process of interest and (ii) an optical signal—exhibiting enhanced interactions with light, giving high contrast. In some cases secondary ligands allow signal amplification. Separating the two aspects of the probe (ligand and signal) allows a chemist to optimise each function. It is sometimes possible to satisfy both criteria with a single chemistry and, more rarely, with a molecule endogenous to the cell. This might be a naturally fluorescent precursor or metabolite, and ring structures found in many drugs impart intrinsic fluorescence.

2. Fluorescent probes

2.1. The ligand or targeting portion of the optical probe

The targeting (ligand) part of the optical probe increases (or decreases) the optical signal by local-

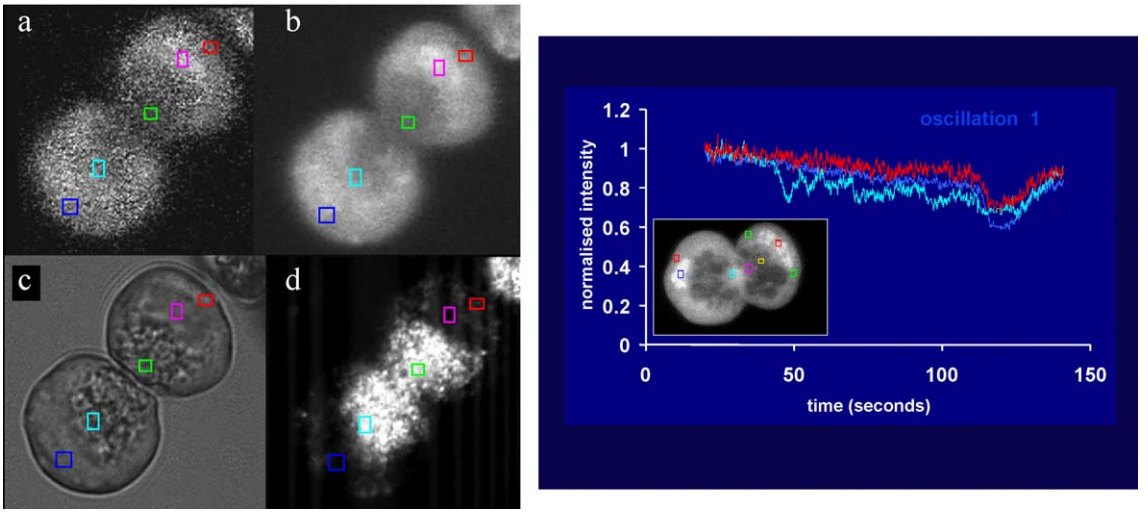

Fig. 3. Fast confocal fluorescence imaging using an AOS scanner. Dual excitation ratio images of Fura-2 labelled pancreatic acinar cells (a,b), phase contrast (c) and confocal reflection (d) images. Long and short-term calcium transients are plotted in the graph for a range of sub-regions in each cell. Courtesy of R.J. Errington and P. Willems, Department of Cell Physiology, University of Nijmegen, The Netherlands.

ising its target by one or more processes including covalent or non-covalent bonding, functional modification or compartmentalisation. Discussion of the range of 'ligands' is beyond the scope of this article but includes chemical agents for covalent coupling of probes to target proteins, non-covalent DNA-binding probes, biotinylation of proteins, antibodies (primary or secondary), ion-binding fluorophores, expression reporters, enzyme substrates, fluorescent protein (GFP)-labelled peptides, etc. Thorough overviews of the range of targeting agents (ligands) available can be found elsewhere (e.g. Refs. [7,8]) and some examples are illustrated in Figs. 2 and 3.

2.2. The signal component of the optical probe

Photochemical probes may use one of several processes to generate optical signal. Cytochemical probes are most commonly absorption stains that produce contrast by absorbing light at certain wavelengths. These types of probe tend to require high concentrations to provide sufficient contrast, are of limited use in living cells but are commonly used on tissue sections. Their absorption of light inherently gives a non-linear response with depth. Surface plasmon resonance can also be used as a photochemical probe where the electron cloud at the surface of metal (e.g. gold) particles scatters light at characteristic frequency depending on size and environment. This is the basis of an important range of non-imaging diagnostic equipment [9–11] and is rarely used in microscopy. Fluorescence is by far the most commonly used and flexible probe signal and is exhibited by a wide range of molecules (Table 1). Image contrast provided by fluorescent probes depends on a combination of absorption and emission. By blocking background auto-fluorescence, a contrast of 10^7:1 or greater is possible. Epi-scopic optics reduce background as most illumination is transmitted away from the lens.

3. The fluorescence process

The physics and photochemistry of fluorescence are well understood and we can look at the process in three consecutive stages: (i) Formation of one or more excited state(s) by absorption (excitation), (ii) non-radiative transitions between excited states and (iii) energy loss accompanied by emission of radiation. These processes are linked reactions, each of which may be described (interchangeably) by statistical probability distributions or reaction rate constants or decay lifetimes, all describing characteristics of the

Table 1
Some common compounds used as signal components of fluorescent probes

Fluorophore	Properties
Fluorescein	Widely used green fluorescent molecule. Well characterised. Excitation around the 488 nm line of argon lasers. Undesirable features; (i) photobleaching, (ii) pH-sensitive emissions, (iii) broad spectrum and (iv) quenching in aqueous environments. Oregan-Green® [7] and Rhodamine-Green, among others, have similar excitation/emission peaks and superior properties.
Bodipy	Useful alternative to fluorescein, with a narrower spectrum (and is thus brighter), greater photostability, insensitivity to solvents, little overlap with red probes and convenient conjugation chemistry. Red emitting versions are available.
Rhodamine	A family of, predominantly, red dyes: Tetramethylrhodamine, lissamine rhodamine and the Rhodamine-X variants (including Texas-Red) are standard red-emitting second probes used alongside fluorescein or its alternatives. Photostable and insensitive to pH but some have complex absorption spectrum around 520–550 nm.
Cy dyes	Range of dyes from Amersham Biosciences, covering UV to NIR. cy2/cy3/cy5 for triple-staining, with many secondary antibodies available.
Alexa fluor®	20+ dyes from Molecular Probes from UV excitation to NIR [7]. Photostable, with less variation to environment or when conjugated to ligands.
Inorganic particles	Quantum dots [68,69] are coated rare-earth microcrystals: spectra depend on their size (a few nm) and chemistry. Lanthanides [70–72] show long lifetime fluorescence and phosphorescence.
Fluorescent proteins	UV, blue, cyan, green and yellow mutants of the *Aequoria* Jellyfish photoprotein GFP. Other mutations alter pH sensitivity, activation (cyclisation) time, thermal stability etc [73–77]. Other marine organisms yield red equivalents-Ds-Red [78] and Hc-Red. 'FlAsH' is a tetra-cysteine motif expressed in a cell by transfection, which is visualised by addition of a fluorescent biarsenical ligand [79].

signal. Understanding these allows us to choose appropriate signals for different tasks. A figure of merit is the ratio of the desired signal vs. all possible reactions (e.g. number of fluorescence photons produced for each excitation photon) called the quantum efficiency (QE) or yield.

3.1. Excitation

Molecules exist with varying levels of internal (potential) energy. Electronic energy levels representing electrons with paired spins are called singlet states. The lowest energy state is the ground singlet and occupancy of all energy levels is described by the Boltzmann energy distribution [12]. However, solvent and other interactions mean that (under biological conditions) virtually all molecules are in the ground state. Transitions between singlet states give excited molecules that might later emit fluorescence. Within each electronic band there are small steps representing bond vibrations and rotations.

Several things may happen, each with a given probability, when a molecule encounters light energy (Fig. 4) each of which has important consequences in biological samples (see also Ref. [13]). Absorption results in increased vibrational and rotational energy of inter-atomic bonds and/or promotion of electrons to higher energy levels (Fig. 3a1). The changes of electron state (transitions) are associated with a quantum of energy and a corresponding wavelength. The probability of absorption at a given wavelength is defined for a 10-mm path length as a molar extinction coefficient. Absorption is linearly proportional to the intensity of illumination for low concentrations and the average time the electric dipole of the molecule is aligned with the illumination electric vector (polarisation). Another important, though rare, outcome is multi-photon absorption where molecules can absorb more than one photon at a time [14,15]. The extinction coefficient or cross section is very small and the energy is coupled into the molecule when photons arrive within 10^{-16}s; a requirement necessitating high illumination levels (Fig. 3a2). Sample illumination can also result in scattering where energy is dissipated (in $<10^{-15}$s) in all directions (Fig. 3b), with a strong inverse relationship to wavelength ($\propto 1/\lambda^4$ for single molecules). Assembly of molecules into large objects, and the electronic environment, can affect scattering, concentrating light in particular directions. Lastly, illumination of a population of molecules of which a high proportion are in a high energy state (a population inversion) can lead to 'stimulated emission' (Fig. 3c). This occurs in lasers and under extreme conditions in fluorescence applications with high light levels [16–18]. Energy is not coupled into the molecule but is released immediately with the same wavelength and phase as the incident radiation. Excited molecules may be depleted by these encounters.

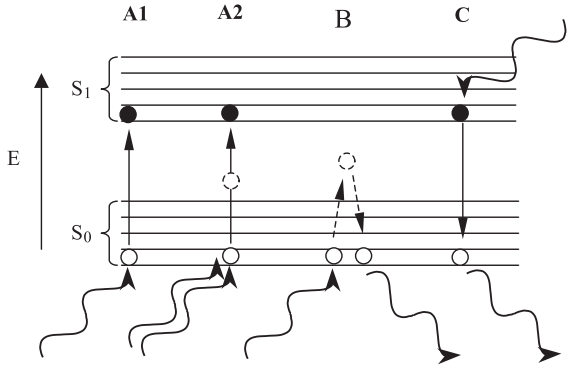

Fig. 4. Energy (Jablonski) diagram for single-photon absorption (A1), two-photon absorption (A2), scattering (B) and stimulated emission (C). S_0=ground electronic singlet state. S_1=first excited singlet state. Several vibrational levels are shown within each electronic band. One or more incident photons may have energy coupled into the molecule, raising its internal energy (A1 and A2), or the energy may be instantaneously dissipated (B) (perhaps via a virtual state) or in exceptional circumstances an excited molecule may be stimulated into releasing its energy, returning to the ground singlet (C).

3.2. Non-radiative excited state transitions

Non-radiative transitions represent important routes to energy states from which energy may eventually be lost from the molecule. For biological fluorescence we need to consider transitions (i) within electronic bands (vibrational and rotational), (ii) between singlet states, and (iii) between singlet and triplet states.

When photons are absorbed, the molecule goes from a ground state to a level within a higher electronic band (singlet). Vibrational or rotational transitions occur (Fig. 5A), with no emission, to the lowest energy state in that band, leaving a molecule with less energy than was absorbed and resulting in emitted light being of longer wavelength. Radiation-

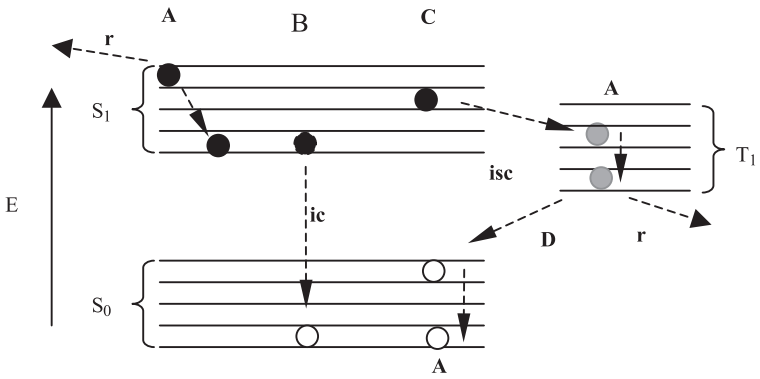

Fig. 5. Energy diagram for non-radiative electronic transitions. T_1=1st triplet state. (A) Vibrational relaxation usually brings excited molecules to the lowest state of a singlet band. (B) Singlet–singlet transitions can occur without emission through internal conversions (ic). (C) Singlet–triplet inter-system crossing (ics) can occur in which energy can be lost from the system by external quenching reactions (r) of singlets or triplets.

less transitions between singlets are also possible, induced by collisions with solvent or other quenching or energy transfer agents, or by vibrational dissipation through the molecule (Fig. 5B).

Each excited singlet has a corresponding 'triplet' state with slightly lower energy. Singlet–triplet transitions happen through a normally forbidden electron spin conversion (inter-system crossing). The energy drop means that transition from the triplet state (e.g. phosphorescence) is always via release of less energy than from the singlet state. Radiation-less transitions from triplet states can occur by vibrational or rotational losses through the molecule. Triplet-singlet conversion (Fig. 5D) has low probability and triplets are long-lived, increasing the likelihood of further reactions—e.g. with molecular oxygen, giving free radical oxygen which is highly reactive to other fluorescent molecules, oxidising them to inactive forms (photobleaching). This is a hindrance in most techniques although it can also be used to investigate molecular dynamics [19,20] (Fig. 5C).

3.3. Emission

Emission represents loss of energy from excited states accompanied by output of radiation (e.g. light).

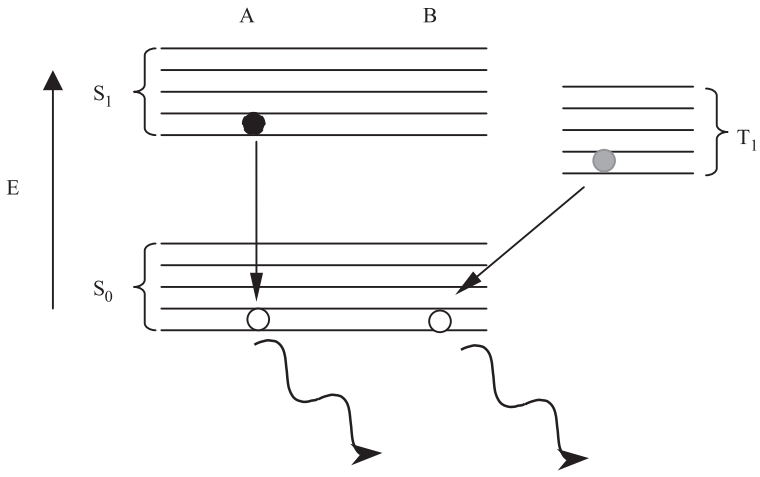

Fig. 6. Radiative energy loss (emission) results in fluorescence (A), usually from the lowest vibrational level of an excited singlet state (e.g. S_1) to the ground state of S_0. Phosphorescence (B) results from emissive energy loss from the lowest vibrational level of a triplet state, e.g. T_1 to the lowest level of S_0.

Two types of emission are important for biological probes: fluorescence and phosphorescence. Both involve the emission of light at wavelengths corresponding to electronic level transitions (Fig. 6).

Fluorescence is exhibited by many biologically relevant molecules as a result of transitions from the lowest level of S_1 following energy dissipation from higher energies. This not only explains the increase in wavelength (Stokes shift) of the emission compared to the exciting light but also often allows us to estimate fluorescence efficiency by measuring the longest wavelength absorption. The rate constants (or probability) of singlets leading to fluorescence yield excited state lifetimes in the range of 10^{-8}–10^{-10} s.

Phosphorescence is the term describing emissions associated with direct triplet to S_0 transitions. These excited states have lifetimes in the range 10^{-6}–10^{-10} s.

3.4. Phase relationships and fluorescence emission

Fluorescence lifetimes represent a statistical overview of a stochastic process, variations within which are slow compared to the rate of illumination (photon flux). This results in a random delay, or phase shift, to the emission (with respect to excitation) and no phase information from the illumination can be recovered from fluorescence. Regardless of the light absorbed (e.g. laser light with high spatial and temporal coherence) fluorescence is always temporally incoherent.

4. Components of a fluorescence instrument

Every fluorescence instrument can be broken down into excitation (illumination), contrast enhancement (e.g. filtration) and emission (detection) parts. In fact, making efficient use of this decoupling significantly enhances some instruments.

4.1. Illumination

We are interested in variations of the biological test system and these must not be overwhelmed by noise in the illumination. Output power is linked with the size of the source. The efficiency with which light can be channelled from source to sample also depends on the wave-front uniformity. The best way of producing an accurate wave front is to engineer a ‘point-source’ but this will emit light in all directions. Spectral character is important in matching the source wavelengths to the energy transitions of the fluorescent molecule(s).

4.1.1. Lamps

Incandescent lamps (e.g. tungsten-halide) have an extended life span by establishing a re-deposition ‘halide cycle’ returning evaporated metal back onto the filament rather than contaminating the glass envelope. DC lamps are stable since the heated filament responds slowly to fluctuations in the supply. Output power (and spectrum) are modified by changing the voltage. The cost of such equipment is low but brightness is very poor at short wavelengths.

Arc lamps, on the other hand, provide better spectral quality. Mercury (Hg) lamps rely on vaporised metal plasma that emits a characteristic spectrum, concentrated in distinct lines that may or may not coincide with energy bands of the fluorescent sample. Hg lamps are at high pressure when running and contain toxic heavy metal. Xenon (Xe) arc lamps are filled to high pressure with that inert gas. Output of Xe lamps is more constant than Hg, with additional spectral lines. Brightness is slightly lower than Hg lamps for the same supply power, and cost is similar (approx. $1 per hour).

Arc lamps must be carefully aligned to avoid uneven illumination. They respond quickly to supply transients, allowing electrical modulation. They have been used with light ‘scrambling’ attachments based on optical fibre delivery, to counter instability and field non-uniformity (see Ref. [21]). New arc lamp systems have recently appeared based on metal-halide technology, with longer lifespan, alignment-free lamp replacement and ozone-free stable output.

4.1.2. Lasers

Lasers are point emitters with output powers limited only by cost and convenience [22]. The lasing process starts with a population inversion of excited molecules by thermal, electrical or optical ‘seeding’ or ‘pumping’ of an emissive material. This may be a crystal, gas or metal vapour, dye solution, semiconductor (diode) or other solid-state material. Emit-

ted light, of a characteristic wavelength, is amplified through repeated stimulated emissions by placing the lasing substance in a cavity formed by two mirrors.

Continuous wave (CW) lasers produce light with a very narrow bandwidth that exits through a partial (output) reflector and may be plane or randomly polarised. Laser light has extremely high spatial and temporal coherence at a resonant frequency, or longitudinal mode, defined by the mirror spacing. Lasers are specified by power (mW) and beam divergence. The transverse beam profile is made up of component transverse electromagnetic modes (TEMs). The resultant is described by an 'M^2' mode number relative to a perfect Gaussian shape (M^2=1−a single 0,0 TEM). Lasers used for microscopy have a beam diameter at their 'waist' (usually near the output mirror) of up to 1 mm.

Pulsed laser illumination (as short as 10^{-11}s pulses) can be achieved by electrical modulation of diode lasers. Mode-locked ultra-fast lasers can deliver kW of power, concentrated into 10–100 fs pulses at 10^8–10^9 Hz (giving average powers up to a few mW). The TiS oscillator is a passive device (requiring no external electrical power), usually seeded by a 3–15 W solid state or ion laser (e.g. at 532 nm). Stimulated emission from a Titanium-doped sapphire crystal in the lasing cavity produces near infrared (NIR) output. Longitudinal modes are combined in-phase where they interfere to form a pulsed output. This 'mode-locking' can be sustained by an acousto-optical modulator (AOM). In addition, or alternatively, the Kerr 'lensing' effect (see Ref. [22]), arising from the extremely high electrical field within each light pulse within the crystal, causes the refractive index to increase, focussing the pulsed component towards the centre of the beam. Adjustable slits block the unfocussed CW light resulting in selective transmission and amplification of pulses through the cavity. A tuneable birefringence filter or prism spectrometer selects the chosen operating wavelength (approx. 700–1000 nm).

4.1.3. Light emitting diodes

Non-laser light emitting diodes (LEDs) produce light in various colours. Their small size (down to 10μm), low power consumption and heat generation, make them ideal sources for compact instrumentation. High brightness is possible in a device costing a few cents per hour. LEDs can be electrically modulated at up to 10^8 Hz.

4.2. Detection of fluorescence

Three questions must be answered when choosing a detector for a given purpose: (1) How much fluorescence do we need to measure? (2) How accurately do we need to measure it? And (3) how fast (frequently) do we want to measure? Fundamental limits within the process of fluorescence provide limiting values for these quantities (e.g. see Refs. [23,24].

How much fluorescence can the probe produce? Time constants for absorption, relaxation and emission mean that bright fluorescence from a population of molecules may last up to around 10 ns. This limits cycling between ground and excited states to 10^7 Hz (photons per second) to avoid saturation (i.e. avoiding generation of a population inversion where more molecules are excited than are in the ground state). A 'good' fluorescent molecule emits 10^4 photons before destructive (permanent) quenching occurs (e.g. by free radicals generated as a by-product of excitation). Thus, we can collect signal using maximum illumination for about 1 s before the probe is destroyed, longer if illumination is decreased further. Assuming a probe concentration of 10^{-6} M starts to self-quench (i.e. inter-molecular reactions remove energy from the excited state without emission of fluorescence), we get an upper limit of 10^6 molecules in a 1 pl volume (e.g. a cell) and a potential total signal of 10^{10} photons per cell. We could generate this signal with maximum illumination at about 10^{13} Hz.

How accurately can we measure the signal? In determining the arrival of a photon at a detector, there is always statistical uncertainty or shot noise, even for a perfect instrument. Under ideal conditions, the noise (and also the s/n ratio) is equal to the square root of the photon count. Our hypothetical cell, labelled with a 1 μM probe, illuminated at maximum intensity, delivers a maximum s/n of 10^5 from a perfect detector. This represents an essentially noise-free measurement. However, we may sample that fluorescence from the cell over its spatial dimensions and/or time, reducing the signal by the number of samples and the s/n by the square root of the number of samples.

How much light can a fluorescence instrument detect? Fluorescence is emitted from the sample in all directions and the highest numerical aperture (1.4 NA oil immersion) objective lens collects only 30% of that light. Absorption and scattering through the instrument optics reduces the signal to 10–80% depending on wavelength (e.g. Ref. [24]). Detector QE will be 10–80% giving a total instrument detection efficiency of 0.3–9%. So we can record 3–200×10^7 photons at 3–200×10^{11} photons per second from our hypothetical cell with s/n of about 10^4:1 at maximum illumination.

We will sample the 10^9 or so photons from the cell as a single measurement or up to perhaps 10^9 samples (e.g. a time series of 3-D voxel images). We must choose between (i) the high s/n (>10^4) of the single sample with no spatial information and (ii) poor s/n (approaching 1) of the 4-D image with high spatio-temporal resolution. Usually a compromise must be made and this juggling of s/n, speed and resolution is the 'eternal triangle' of fluorescence imaging.

4.2.1. Photo-detectors

Light falling onto the photo-material of a detector is either absorbed or scattered. Absorption can heat the detector and/or the charges within the material may be altered, generating an electrical signal [25]. Detector QE is the ratio of photons absorbed to photons producing detectable signal. Other noise sources can be significant. If the charge carriers stay within the material, photovoltaic or photoconductive detection are possible. External or photo-emissive detectors, where electrons escape from the surface, are important for fluorescence work.

Photoconductive detectors make use of the process by which photons produce electron-hole pairs directly (intrinsic) or in an area of impurity (extrinsic). The majority population of charge carriers results in an electrical signal.

Photovoltaic detectors make use of free electron-hole pairs, produced by incident photons, in an applied electric field. 'True' photovoltaic detectors operate with no bias voltage but are usually reverse-biased and a resulting photocurrent measured (Fig. 7a). Minority and majority carriers are required for an intrinsic photovoltaic effect and the shorter lifetime of minority carriers gives a higher frequency response than photoconduction. Another advantage is the

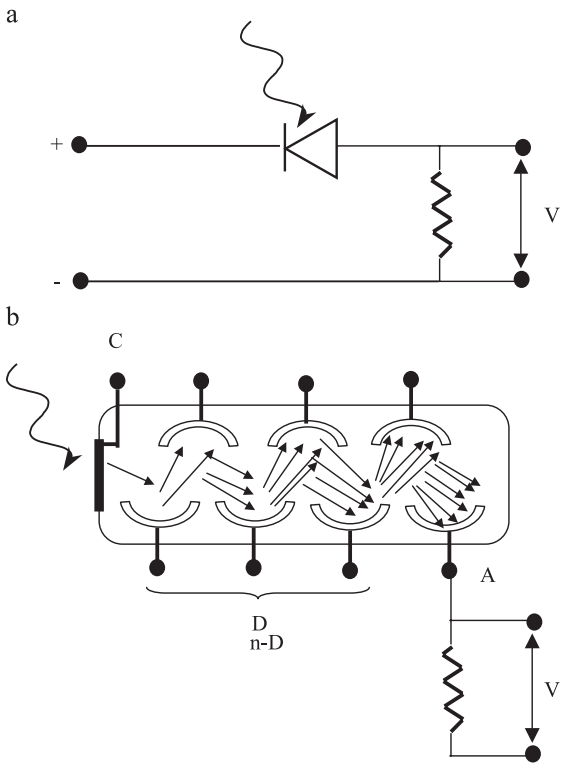

Fig. 7. Simplified diagrams showing generalised configurations of photodiode (a) and photomultipler tubes (b). Photo-diodes (a) are usually operated in the photovoltaic mode where an applied field results in free electron-hole pairs in the device in response to incident light. A photocurrent is measured under reverse bias conditions, giving a higher frequency response than is possible with a simple photoconductive circuit. Photomultiplier tubes (b) are the most common photoemissive devices. Light falling on the photo cathode (C) produces secondary electrons that are accelerated and amplified by a series of dynodes (D) at increasing potential. In analogue mode the PMT signal is measured as a photocurrent at the anode (A).

ability to introduce gain within the device by allowing electrons produced by incident light to collide with atoms to produce secondary electrons in a cascade or avalanche. This cannot improve the detector s/n (the QE is unaffected) but the output can be large enough to make noise in subsequent stages insignificant. A disadvantage is the special driver needed that rapidly switches between sensing, readout and recovery, requiring a fast quenching circuit to remove charge before the next detection.

Photo-emissive detectors work by ejecting electrons from the detector surface, where external avalanche methods of generating gain become possible. A photo-

cathode emits an electron (when a photon is absorbed) that is collected by an anode. Gas filled phototubes provide avalanche gain by collisions with the gas molecules. Photomultiplier (PMT) tubes use a series of dynodes to accelerate electrons by several avalanche bursts towards the anode (Fig. 7b). These detectors are fast, with sufficient gain to make subsequent noisy stages irrelevant and operate at high repetitions (10^8 Hz). Photo-emissive material coated inside a capillary tube is the basis of the micro-channel plate (MCP). An electric field applied along the tube accelerates photo-electrons, generated at one end, producing secondary gain electrons. The tubes are stacked horizontally into a plate. One or more MCPs can be placed in front of a detector to increase the signal. The achievable QE is that of the photocathode (10–25%, or up to 40% for GaAsP devices) and not the final detector material. MCPs can be used as an external avalanche chain in an extremely fast MCP-PMT, although the high fields make these devices very sensitive to damage.

4.2.2. Non imaging detectors

Some instruments measure fluorescence over time without sampling (imaging) spatial frequencies. Often, a single detector is sufficient and efforts can be focussed on the sensitivity and temporal response of the device. Avalanche photodiodes (APDs) are useful at modest repetitions (kHz), e.g. for fluorescence correlation spectroscopy, although the gain and sensitivity vary over the surface so they are small and the detected beam must be stationary. PMTs or MCP-PMTs, though larger and more expensive, are better for high sensitivity, high frequency (MHz) applications.

In some applications 'non-imaging' detectors can be used to generate an image. Diode or CCD arrays with thousands of elements are used in some cameras to build a 2-D image by scanning the array through the image-plane. Other scanning configurations can be used with a non-imaging detector, such as a PMT, to produce images. Small arrays can also be accurately 'over-scanned' to generate larger images.

4.2.3. Sampling or imaging detectors

It is sometimes desirable to form an image optically and then measure the light distribution using an array or imaging detector. Photographic materials, based on silver-halide and/or photo-dye chemistry have, until recently, produced superior results for low-light work including fluorescence. This is due to the small grain size (a few micrometers) possible in photo emulsions and the relatively slow development process. Digitisation of films by scanning (for computer processing or analysis) introduces its own problems of convenience and time-scale. Photoconductive or photovoltaic methods can be used in devices capable of being stacked into imaging arrays. Linear arrays of regular photodiodes are used in 1-D applications but they have limited practical use as 2-D arrays. Cost and size tend to prohibit the use of arrays of photo-emissive devices, although a 'multi-PMT' module with up to 16 channels has been developed by Hamamatsu which uses shared components to make a useful multi-channel detector [26].

4.2.4. CCD arrays

Charge-coupled devices (CCDs [25]) solve many problems of diode arrays. Similar internal photo-effects are used to generate electrons that are injected into capacitor arrays, created on the device by metal-insulator-silicon (MIS) or metal-oxide-silicon (MOS) technology. Charge accumulates in these 'potential wells' at about 600 electrons per square micron, is moved between wells by phased signals applied to each electrode and converted to an analogue or digital signal at the edge of the chip. The high QE of silicon in CCDs is offset because the wells do not cover the entire chip surface, and the front portion of the chip contains components that block light, reducing sensitivity. To counter this, the back (support) side of the chip can be thinned to make it transparent and back-illumination used, improving QE to around 85%. Extra gain can be added by an avalanche-intensifier in front of the chip (e.g. MCP, vacuum tube, etc.). Alternatively an APD-type approach can be employed where electrons are accelerated to secondary collisions within the chip, giving a sensitive CCD with variable gain.

4.2.5. Sources of noise

Signal processing electronics can be designed to add little extra noise, so under moderate–high light conditions, s/n is limited by detectors. Thermal effects from absorbed photons and the operating temperature introduce unwanted background, increasing over time, and can be partly countered by subtraction of a mean dark signal. This only removes the constant (DC)

component. Cooling of the detector, by a heat sink, Peltier-effect device and/or cryo-cooling (e.g. liquid N_2) reduces all frequencies of background, e.g. to less than 0.01 electrons per pixel per second in a good CCD. Thermal effects are seen in PMT and APD devices and they can also be cooled. Some avalanche electrons are not correlated with incident photons so these devices also generate internal noise.

4.2.6. Photon counting

In low-light applications, the main source of noise is the statistical uncertainty in the number of photons detected. Any noise in the detectors or electronics is significant. An ideal solution is to count photons, rather than produce a photocurrent in proportion to their arrival rate. This removes instrument noise and simplifies quantification and calibration. Many avalanche devices can be operated as photon-counting devices, provided the charge is amplified sufficiently to overcome the read-out noise. A fast response is required, so a photo-emissive device (e.g. PMT or MCP-PMT) is normally used, operated at a voltage pre-set to produce the maximum s/n at low photon flux. Pulses are produced at the detector output and counted if they exceed a pre-set level (depending on the characteristics of the detector). Small amounts of noise have no effect on the counter and it is possible to correct for pulses from multiple-photons provided the device is operated at a low enough photon flux. For a typical PMT, at 10–20 MHz, about 50% of the photons might be miscounted and a linear response obtained at a few MHz.

4.3. Which detector?—'Horses for courses'

CCD arrays are universally used where a complete optical image must be digitised. They have a good QE (up to 85%) so are efficient detectors and devices are available with pixels of various sizes to suit the image size and signal level of most applications. The major disadvantage is the high read-out noise, particularly when CCDs are read-out rapidly (>1 MHz). Avalanche gain enhancements raise the signal above the read-out noise making these intensified CCDs suitable for faster imaging or low-light applications. When imaging is not required, or scanning is employed, highly efficient photo emissive devices like the PMT provide almost noise-free gain, regardless of the detection speed. Scanning implementations (such as LSMs) have the disadvantage that data is produced serially and so the speed of acquisition is limited compared to what is possible with imaging array detectors. With samples showing significant movements (e.g. living preparations) the relative advantages of array detectors over non-imaging detectors with scanning are not always clear. Since light is collected in parallel over the entire CCD chip during each frame exposure, image blurring will occur if movements occur significantly during the each frame time. For a scanning beam, movements of small objects will only show blur if they are significant while the beam scans across their dimensions. Frame-to-frame movements of small particles will show up as a geometric distortion of their positions, rather than a blurred image.

Resolution is primarily determined by the optics of the instrument. This is modified by the size of the pixel array in an imaging CCD. In order for this not to be limiting, at least 2.3 pixels should be used to cover the distance equivalent to the airy-disk FWHM at the image plane.

5. Measuring the fluorescence process

We can describe various parameters, characterising the fluorescence process.

5.1. Fluorescence intensity

Signal intensity relates to the averaged output of excited states that decay by fluorescence (Fig. 8A). Calibration is required to infer the probe concentration from intensity. Many uninteresting aspects of the probe (e.g. variations in concentration, sample thickness, photo-bleaching, etc.) can mask important features of the labelled target. As a control, we collect a reference signal from another probe or at a different wavelength (e.g. see Ref. [26]). The reference must behave like the probe in terms of the uninteresting properties and in a contrasting or neutral way for the desired properties. The ratio of probe to reference (after subtracting background) gives a value more closely related to the concentration of the target (e.g. Figs. 2 and 3).

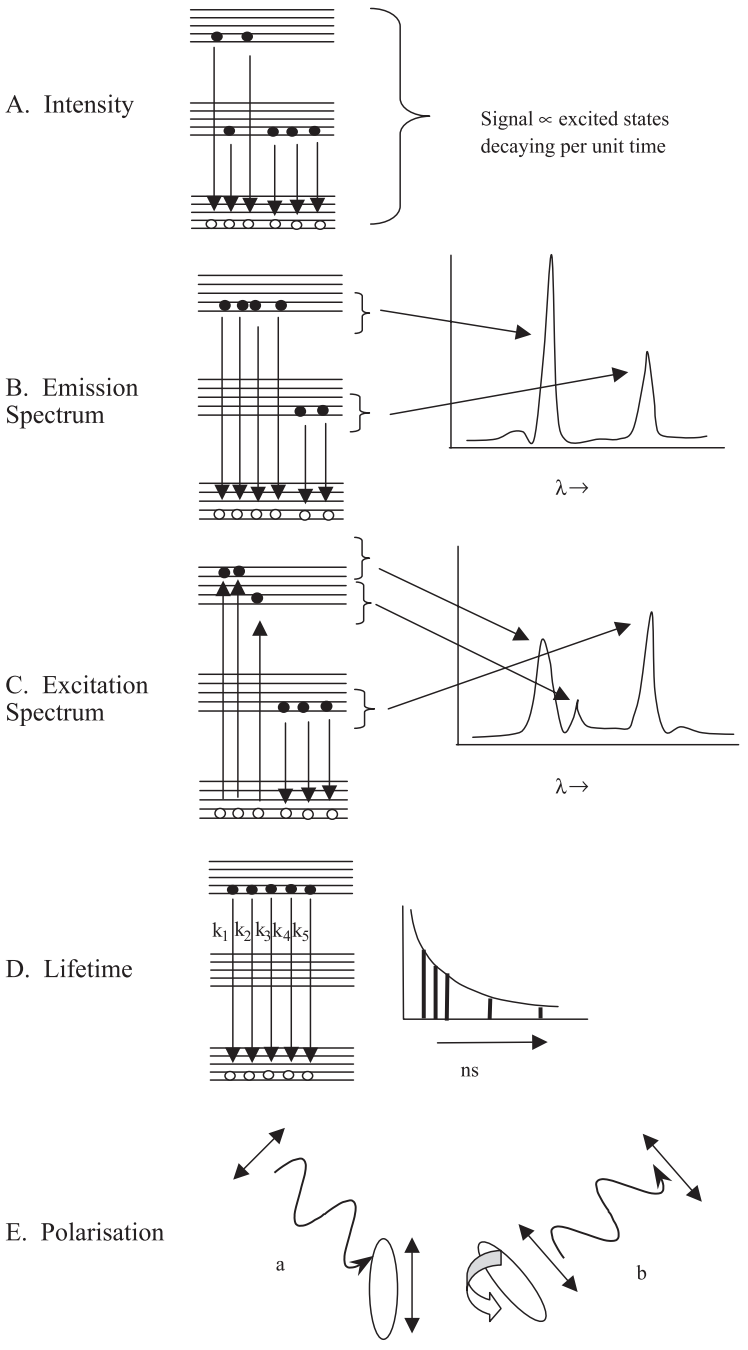

Fig. 8. Diagrammatic representation of the different measurable aspects of the fluorescence process. Each describes a key parameter of the underlying photophysics. Intensity (A) is simply the average contribution from decaying excited states. Peaks in the emission (B) and excitation (C) spectra indicate key energy transitions of the population of excited molecules. Lifetime (D) represents the contributing decay times for each of the molecules of the population which together, give the characteristic exponential decay curve. Polarisation (E) describes how the electric vector of the illumination can excite fluorescence if it is partly aligned with the electric dipole of the molecule (a), molecular rotation between excitation and emission will result in a change in the polarisation of fluorescence (b), compared to the illumination.

5.2. Fluorescence spectra

Fluorescence emission (Fig. 8B) and excitation spectra (Fig. 8C) reflect the range of energy gaps associated with excited states of the probe(s) and are sensitive to the electronic environment. An emission spectrum can be made by passing the light through a prism and recording the resultant 'rainbow' using a detector array (e.g. see Ref. [26]). Alternatively, one or more spectral bands may be isolated using interference filters, adjustable slits in a prism or grating spectrometer, or a liquid crystal tuneable filter (LCTF). Multiple probes with distinct spectra can be measured in this way. Spectral reassignment software is used to separate probes with overlapping spectra. Success in this technique requires low noise data and may require good reference spectra.

5.3. Fluorescence lifetime

The lifetime measured for a given probe is the time constant, τ, of the exponential fluorescence decay of the population of molecules measured. It reflects the rate constant of the transition to the ground singlet state as well as the time-averaged concentration, proximity and orientation of agents that can alter the decay of the excited state(s) (Fig. 8D) [27]. It is independent of the probe concentration (in the absence of self-quenching). Lifetime is measured by either (i) modulating the illumination and detection and measuring the signal while changing the phase difference between them [28] or (ii) time gated (e.g. Ref. [29]) or correlated detection, often with single photon counting (e.g. Ref. [30]). In this method, the arrival time of photons with respect to a pulsed illumination source (0.1–50 ps pulses at up to 100 MHz) is measured.

5.4. Fluorescence polarisation

Orientation of the electrical dipole of a molecule at the time of absorption determines the polarisation state of excitation. During the short, but random, lifetime of the excited state a molecule may rotate (Fig. 8E) giving an emission with a different polarisation [31,32]. By measuring the randomness of this depolarisation (fluorescence 'anisotropy') the mobility or diffusion characteristics of the molecule can be estimated [33]. These parameters are largely independent of the probe concentration.

5.5. Photo-bleaching and photo-activation

Reaction rates or lifetimes for destructive quenching can be determined as a rate of photo-bleaching. By measuring fluorescence recovery after photo-bleaching (FRAP) [34] or fluorescence loss in response to photo bleaching (FLIP) [35], molecular mobility can also be determined [36,37]. In FRAP, non-fluorescent molecules move into a region of the sample previously bleached with high illumination. The FLIP alternative simultaneously measures intensity loss from a region neighbouring the bleached area.

Some molecules and complexes can be designed to fluoresce only after pre-illumination (photo-activation) at an appropriate wavelength [38–40]. This may be a rearrangement of a non-fluorescent molecule to a fluorescent form or a quenching agent may be removed or modified by photo-destruction.

5.6. Fluorescence correlation spectroscopy (FCS)

Fluorescence intensity, over time, shows variations due to molecules moving in and out of the beam as well as orientation effects. These average out in a large population so very low s/n is achieved. Information is extracted by auto-correlating the signal (searching for repeats) from a focussed spot over time. As the number of molecules is reduced, s/n increases, thus FCS is useful for examining mobility of low concentrations, even single molecules, including binding and release at surfaces (e.g. [41–43].

6. Fluorescence instruments

Each of the configurations described below are capable of operating in all modes discussed above. We will explore key features and their use.

6.1. Non imaging instruments

Fluorescence devices that cannot sample over spatial dimensions are typically used for measuring concentrations, molecular dynamics and associations or configurations. Such devices include fluorimeters,

micro-plate readers and flow cytometers. Analytical fluorimeters typically use arc lamp and/or laser illumination with filters or a monochromator selecting wavelengths to illuminate a quartz cuvette and detect fluorescence using one or more PMTs. Scanned excitation/emission wavelengths provide high-resolution spectra reflecting energy transitions of fluorescent molecules. Fluorimeters can be used to measure fluorescence in solutions, cell suspensions or cells on covers glasses and adaptation of this technology allows fluorescence sampling of multi-well plates in micro-plate readers. Fluorimeters measure averaged fluorescence in a cell population, which will mask differences between individual cells. This sampling problem can be avoided by using a flow cytometer, which is essentially a fast fluorimeter with a sequential single-cell multi-sample chamber [44]. A jet of medium containing cells streams past a high NA lens. A light source (usually laser) excites fluorescence in each passing drop, to be collected by a sensitive PMT. Individual cells are represented in a scatter-plot of intensity in each of several fluorescent channels and analysed to classify their physiology, biochemistry, cell cycle state, etc. Flow cytometry can analyze up to 10^9 cells per second and 'sorting' systems can deflect each cell into a selected receiver using criteria determined from the measured signal(s).

6.2. Imaging instruments

These instruments produce a spatially sampled array or 'map' of fluorescence. Images may be produced by the optical system directly or built up by scanning.

6.2.1. The fluorescence microscope

Illumination wavelengths (from an arc lamp) are selected by an excitation filter or spectrometer and the light is spread onto a field aperture by a high NA condenser lens. It then reflects from a 45° dichroic mirror and an image of the field aperture is demagnified into the sample by an objective lens (Fig. 9) [45–47]. In this way, the entire sample is evenly bathed in light. Fluorescence is collected by the objective and forms an image in the microscope that is either inspected visually, using a magnifying eyepiece, or passed to an appropriate photo-detector such as a CCD camera (e.g. image 1). All parts of the illuminated sample contribute to the image that contains sharp (in focus) features as well as out-of-focus features.

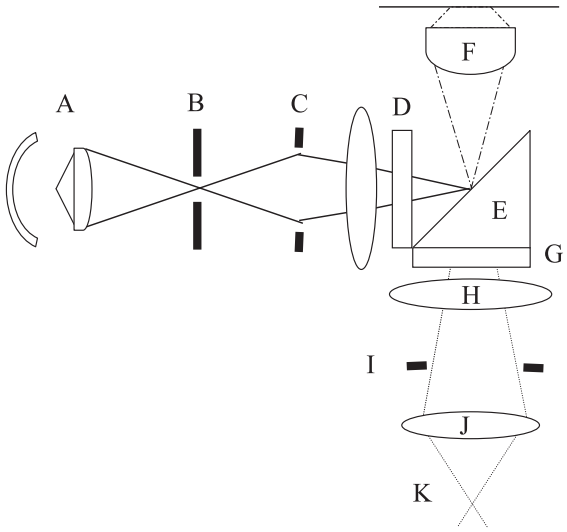

Fig. 9. Simplified form of a basic fluorescence microscope. Arc lamp illumination (A) is focussed by a collector lens onto an aperture diaphragm (B) and is consequently spread out evenly over the field diaphragm (C) (an image plane). Excitation wavelengths in the light from the field diaphragm are selected by a filter or other device (D). A dichroic mirror (E) reflects illumination into a high NA objective (F) which produces a demagnified image of the field diaphragm within the sample. Fluorescence (dotted lines) from the sample is collected by the objective, filtered by the dichroic and emission filters (G) and forms an image (I) at the primary image plane by a tube lens (H). A camera can be placed at (I) or an eyepiece (J) can form a parallel beam converging at a virtual pupil aperture (K) for viewing by eye.

It is important to consider the performance characteristics of fluorescence microscopes. An image of a sub-resolution fluorescent bead (i.e. smaller than about 200 nm) will show an airy disk consisting of a central spot surrounded by faint light and dark rings (e.g. Ref. [48]). Measurement of the airy disk gives parameters describing the microscope performance. The distance from the centre to the first dark ring describes horizontal (x, y) resolution and is given by:

$$d_{xy}\frac{0.61\lambda}{\mathrm{NA}} \tag{2}$$

Where NA=the numerical aperture of the objective lens; λ=Wavelength of the emitted fluorescence (see also Refs. [24, 48]).

To take account of the emission spectrum of a real molecule, contributions from all wavelengths should

be considered. However, the resolution (in fluorescence) is independent of the illumination wavelength and the objective magnification. If a focus series of images of the bead is collected, the corresponding axial (z) resolution is:

$$d_z = \frac{3.27 d_{xy}}{\mathrm{NA}} \eta \quad (3)$$

where η=refractive index of the sample medium.

This is significantly worse than in the horizontal plane and depends on the square of the NA. Total intensity in any horizontal plane is proportional to NA^2/(magnification) and is constant near the focus, so there is no optical sectioning in a conventional microscope.

6.2.2. Scanning optical microscopes

We can first consider reducing the illumination aperture of a conventional microscope to a tiny point. Instead of the whole specimen being bathed in light, a 'double-cone' of focused light is centred on a single point in the sample. We might scan the aperture across the field [49], which will in turn scan the focussed spot through the sample, collecting light visually or into the CCD array. The airy disk image will be similar to that of a conventional microscope but there will be an equal contribution from both excitation and emission wavelengths. Alternatively, intensity can be integrated over the entire CCD array or collected into a non-imaging detector (e.g. a PMT) for each point of the scan. This gives a significantly different result. Fluorescence is no longer imaged at the detector, the objective gathers light from the entire sample at each point in the scan. However, the excitation is imaged to a point that is scanned through the sample. The airy disk is smaller than in the conventional case, depending on the Stokes shift of the probe, as resolution now depends on the wavelength of excitation only (λ in Eq. (3)). The fluorescence emission spectrum is now irrelevant to the resolution. Contrast in this scanning optical microscope [50] is improved since the focussed illumination does not excite other areas of the specimen as each image point is collected.

Various scanning methods are available for optical systems using lasers and non-laser sources.

6.2.3. Aperture scanning

Commercial versions of a scanning aperture include the spinning (e.g. Nipkow) disk systems with spirals of small holes that sweep out the illuminated field [51]. Various hole patterns have been used. A drawback of all these designs is that to prevent illumination from one spot overlapping another, the holes must be spaced far apart, limiting transmission through the disk. This system can be used with arc-lamp illumination but the efficiency is low. A variation (e.g. Ref. [52]) uses two disks, one carrying the apertures and a preceding disk with tiny microlenses over each hole. This enables more of the disk surface to capture light as each lens focuses light through the corresponding aperture. New devices, such as the optical array scanner, with no moving parts, allow fast aperture scanning in the excitation and/or illumination paths.

6.2.4. Stage scanning

Although slow in comparison to other methods, stage scanning has the advantages that the light beam is stationary and the optical path is simple [50,53]. This on-axis route through the lens imparts the least aberrations and the scanned field size is independent of the lens magnification. This is the only method that allows low magnification images to be collected with the highest NA objectives.

6.2.5. Beam scanning with mirrors

One or two galvanometer-driven mirrors can be used to impart a rectangular scan to a laser beam [54]. Optically simple schemes include a single mirror, but this is difficult mechanically, or 'close-coupled' mirrors (with no intervening optics) that do not produce an ideal scan. Optically coupled mirrors can be separately controlled allowing zoom, pan and scan rotation but a difficulty with this scheme is to find an efficient method of transferring the beam from one mirror to the other. Lenses introduce aberrations, but high quality mirrors minimise many errors.

6.2.6. Acousto-optical scanning

This is a method capable of scanning a laser beam at MHz frequencies, e.g. for video-rate (or faster) imaging. An acousto-optic scanner (AOS) contains a crystal (similar to the AOM) which is

optimised to deflect the illumination beam [55] (e.g. Fig. 2). Changing the phase of the driver signal produces a variable deflection. Changing amplitude alters transmission. Two challenges with this device are that the beam shape is distorted, requiring correcting optics, and the system is difficult to implement accurately for several simultaneous wavelengths, making de-scanning and multiple-wavelength excitation difficult.

6.2.7. Line scanners

Instead of scanning a point through a 2-D raster, great improvements in speed can be gained by generating a focussed line and scanning this in one axis. The system is rather like a wide-field imaging device in the *x*-axis and a point-scanning device along the *y*-axis, with intermediate optical performance. Sensitivity is improved over a true point scanner, as many points along the line can be detected simultaneously using a CCD array.

6.2.8. Fast scanning methods

Both the aperture scanning disk system and the AOS can generate a scan fast enough for framing rates of over 100 frames per second (fps) (Fig. 2). Mirror scanners for the fast *x* line-scan have the problem of significant inertia that limits the acceleration, and hence the speed at which they can scan back and forth. The driving signal is usually a saw-tooth waveform so that fluorescence is detected during the left-to-right scan, for example, with a fast 'fly-back' from right to left. Speed increase is possible by scanning and collecting data in both directions, so called 'bi-directional scanning'. Absence of a fast fly-back reduces the acceleration/deceleration forces allowing faster than two-fold increase in scanning by this method and rates of 2000 lines per second (or more) are possible. An alternative approach is to use resonant scanners operating at a frequency where significantly more energy can be coupled into movement. This permits faster scanning, at the expense of more features such as continuously variable zoom, pan and rotation of the scanned region.

6.2.9. De-scanned detection

With an efficient scanner, the emission from the scanning spot can be de-scanned so as to regenerate a stationary beam (Fig. 10). An obvious benefit of this for the LSM is that a smaller detector can be used at the image plane and spatial filters can be used to modify the de-scanned beam point by point. The stationary beam is particularly important for detectors where the performance varies with position on the detector surface.

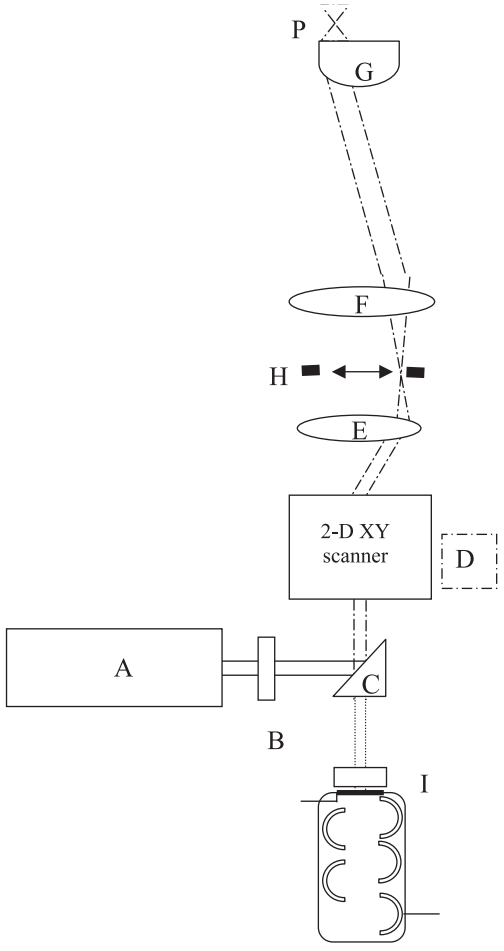

Fig. 10. De-scanned detection. The dichroic reflector separating the illumination and detection paths (C) is placed before the microscope optics, rather than within them (as in a conventional instrument). Laser illumination (A) is filtered (B) and scanned (D) into the microscope to produce a demagnified image in the sample of a 2-D point scan in the primary image plane (H). Fluorescence from the sample is re-imaged at (H) and then passes back through the scanner to a stationary beam which is passed to a non-imaging detector at (I). The scanner both generates the scan and descans the returning beam to simplify the detection optics in the laser scanning microscope.

6.3. The confocal spatial filter

The commonest spatial filter in an LSM is a small aperture in the image plane of the de-scanned emission path (Fig. 11, [55–58]). This is the principal of co-focussed (or confocal) illumination and detection. Excitation and emission optics each have their own imaging response, (see Eqs. (3) and (4), substituting the appropriate λ). The resultant confocal response is the product of these components, which has important results for performance. The confocal arrangement has imaging properties that depend equally on the illumination and detection wavelengths. If the confocal aperture is progressively opened, the contribution of the emission decreases until the performance is that of the simple LSM we first described.

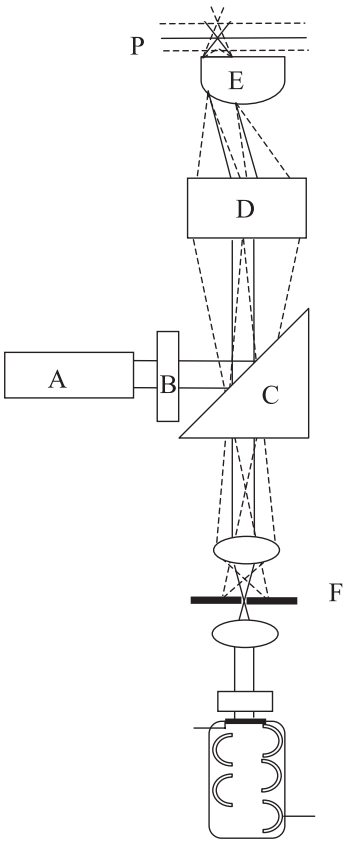

Fig. 11. The confocal spatial filter. Light emanating from the centre of the focussed illumination spot (P) in the sample (solid line) is brought to a focus (F) either by a pair of lenses or by having a long optical path and using the natural 'waist' of the Gaussian beam. A pinhole at this focus, equivalent to (i.e. 'confocal' with) an image plane, blocks light from above and below the focal plane in the sample (dotted lines). When the focussed spot is scanned, an 'optical section' is swept out in the sample. The thickness of this section depends on the relative size of the confocal pinhole.

6.3.1. Resolution and optical-sectioning in the confocal LSM

Any dependence of the confocal geometry on the emission wavelength might seem a disadvantage but this is offset by the co-operative effect of the excitation and detection responses. The distance from the airy-disk centre to the first dark ring is slightly greater than for the non-confocal case while the width at half maximum height (FWHM) of the central peak is about 1.4 times better for a fluorescent probe with small stokes shift [24]. The FWHM of the central peak along the z-axis in a confocal microscope is up to 1.4 times better than an LSM with wide-field detection and the centre to first dark ring distance is slightly greater.

The total integrated image intensity in any horizontal plane is not constant for a confocal microscope (Fig. 12) [56]. A photon arriving at the detector must have been both generated by the exciting light and passed through the confocal aperture. This makes the probability of obtaining a contribution to the image from progressively further away from the focal plane fall off in inverse proportion to the square of this distance. In this way, the confocal aperture blocks light from outside the focal plane giving an image composed of in-focus light called an optical section (e.g. Figs. 2 and 3). The thickness of this optical section is approximately the same as the axial resolution.

6.3.2. Signal level in the confocal LSM

The confocal aperture obstructs much of the fluorescence that might otherwise contribute to the image which often results in a large reduction in signal level (see $\sum I_z$ plots in Fig. 12), but it should always be remembered that it is out-of-focus light that is blocked and so we should consider the signal level from features within the optical plane in terms of the loss of useful information. Reduction of background is as important as overall signal level in determining s/n ratio and the confocal microscope selectively blocks out-of-focus background, therefore s/n is improved as

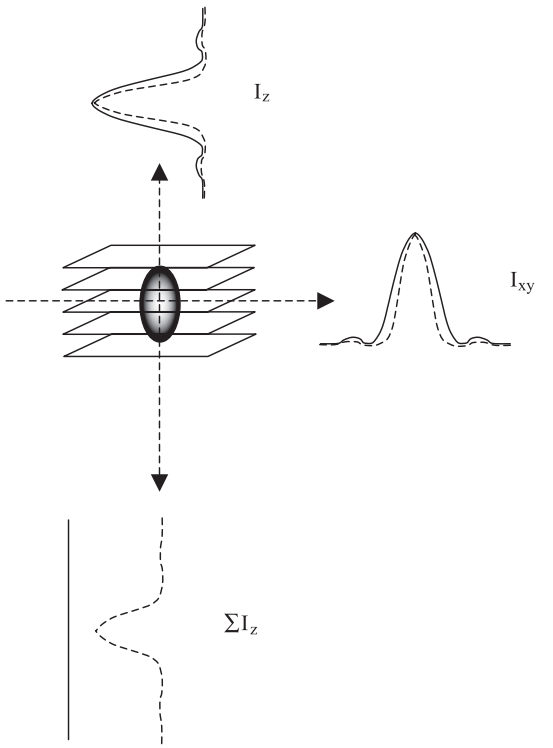

Fig. 12. Geometry of the focussed spot in a laser scanning microscope. If images of a sub-resolution (e.g. 50 nm) fluorescent bead are taken at intervals along the z (focus) axis: the lateral profile (I_{xy}) plot for a confocal microscope (dotted line) will show a central peak about 1.4 times smaller than a non-confocal single-photon system (solid line). This is also true for a line plotted along the z axis (I_z). Integrating all the intensity in each image plane and plotting against z ($\sum I_z$) shows a peak around the central section for confocal (dotted line) images but no significant contrast in Z for conventional data (solid line).

the detector aperture is reduced. At the point where the loss of overall signal equals the rejection of background a minimum aperture size is reached. This position depends on the sample thickness and how strong the out of focus contributions are. The usual practice is to set the aperture to an optimum size, no smaller than about half the diameter of the first airy disk dark ring.

6.3.3. Depth penetration in the confocal microscope

Samples scatter illuminating light and also produce blurring in a conventional image as the light scattered (even from the in-focus plane) appears to emanate from out-of-focus regions. A similar effect happens when a high NA oil immersion lens is used with an aqueous mounted specimen, in this case because the light no longer propagates as a spherical wave to a point focus. Confocal microscopy removes out-of-focus light, improving contrast in images of thick specimens and tissues. However, the scattering and spherical wave aberrations result in a progressive attenuation of signal with depth into the specimen as the aperture blocks these defocused contributions. The problems are particularly acute for very short wavelengths especially ultra-violet excitation.

6.4. Multi-photon excitation

Multi-photon excitation [14,15] delivers optical sectioning by illumination alone, and is best implemented with non-confocal or wide-field detection. Fluorescence excitation falls off as the inverse square of the distance away from the focal plane, achieved by arranging for molecules to absorb two or more photons simultaneously (i.e. within 10^{-16} s). Although the process works for photons of different energies, it is usual to operate with the laser set at a single wavelength. Two photons of any wavelength have the combined energy of a single photon of half that wavelength. Fluorescence molecules normally excited at about 350–500 nm have two-photon excitation at near-infrared wavelengths of 700–1000 nm [59]. Three-photon excitation at these wavelengths corresponds to single-photon absorption around 230–330 nm.

One way to understand how illumination power affects two-photon absorption is to imagine throwing many dice in order to obtain a result of two sixes. If the dice are thrown two at a time the probability of getting two sizes is $(1/6\times1/6)=1/36$, i.e. the product of the individual probabilities of getting a single six. If the same number of dice were thrown four at a time this increases to 1/15 per pair and for handfuls of 8 dice this further improves to 1/10. For very unlikely events, such as two-photon absorption, the effect is more marked. The best strategy for improving the efficiency of multi-photon excitation is thus to ‘throw’ the photons in batches, i.e. to use a pulsed light source. The high photon density (light level) required to achieve realistic signal levels for biologically relevant molecules is only possible with ultra-fast pulsed lasers.

6.4.1. Optical performance in multi-photon fluorescence

The excitation version of Eqs. (2) and (3) gives the resolution and sectioning power of the multi-photon LSM. The probability of two-photon absorption is proportional to the square of laser power so the square of Eqs. (2) and (3) describe the excitation. We might expect the size of this function to show a central peak that is 1.4 times smaller than that found for the non-confocal LSM but the excitation wavelength is twice (for two-photon) that of the single-photon case for the same energy transition(s) of the probe. We thus see a 1.4 fold increase in the FWHM over the simple LSM, but a smaller increase over the equivalent measure for a regular microscope (depending on the Stokes shift). The airy-disk is approximately double that of a confocal microscope for probes with a small Stokes shift and less for longer wavelength emissions. For three-photon processes (at three times the wavelength) the FWHM of the fluorescence response is 2.4 times larger than a simple LSM but only 1.7 times that of the single-photon confocal response. A three-photon optical section is about 2.7 times as thick as a single photon confocal section. All the multi-photon results can, in principle, be improved by a further factor of 1.4 by including a confocal aperture. This approach is not usually employed due to the unavoidable signal loss and the decrease in depth penetration into thick specimens.

6.4.2. Laser power and multi-photon excitation

Selection rules for electronic transitions in the fluorescent molecule make three-photon processes more likely than we might otherwise expect and the proportional increase in laser power required for three-photon excitation compared to two-photon is much less than that needed for two-photon over single-photon absorption. This means that three-photon processes, particularly of intrinsic (auto fluorescent) cellular species, cannot be ignored in two-photon excitation, especially when using sub-100 fs ultra-fast lasers. The relationship between multi-photon fluorescence and illumination is:

$$I = \alpha \frac{P^n}{(\omega r)^{n-1}} \tag{4}$$

where I=fluorescence intensity for n-photon absorption; α=n-photon cross section; P=average illumination power; ω=width of laser pulse; r=repetition rate of laser pulses.

The $(n-1)$ order of the denominator is called the 'short pulse advantage' and would, in the absence of other effects, demand use of the shortest possible pulses. In practice, the wide bandwidth of an ultra-fast laser means that dispersion (variations of refractive index with wavelength) in the microscope optics will cause very short pulses to be spread out in time. The optimum laser pulses, for a typical multi-photon microscope, are just over 100 fs.

6.4.3. Advantages of multi-photon excitation

Since the optical performance of multi-photon microscope is typically inferior to confocal microscopes we must look at areas other than resolution to see the benefits of multi-photon methods. These mainly stem from the fact that the focussed last beam passing through the sample is composed of NIR light at wavelengths above 700 nm. Since scattering of light by has a strong dependence on wavelength ($1/\lambda^4$) the use of NIR light allows excitation and imaging deep within tissues which are obscured by light scattering in single-photon microscopy (e.g. Ref. [60]). Scattering of emitted light does occur and impairs detection, but the effect of this is lessened by the use of a large-area detector, since there is no need for descanning and focussing on a confocal aperture. In many applications the use of multi-photon microscopy avoids photodamage since only the thin optical section at the focus of the beam encounters light energy equivalent to UV or blue light. This effectively limits photobleaching or phototoxic effects, which occur throughout the cones of illumination in single-photon imaging. This is particularly advantageous for UV-excited dyes since high energy UV light is most damaging to cells [59]. Images illustrating applications of multiphoton microscopy are included in other papers in this issue of Advanced Drug Delivery Reviews [59,60].

6.5. PSF engineering

Modifying the size and shape of the LSM 3-D airy disk (called a point response or spread function or PSF) is an example of what can be termed 'PSF

engineering'. Several sophisticated manipulations of the LSM PSF have been attempted. These include the 'Theta Microscope' (e.g. Ref. [61]), which uses up to four excitation and emission beams intersecting to give a near spherical PSF with the same resolution in all axes. The '4-Pi' LSM [62] uses two phase-locked illumination beams at 180° to generate a smaller centre to the airy disk. A particularly elegant method is the use of photons of two different energies in a multi-photon process. The PSF generated by one wavelength is made smaller by depleting the excited states it produces in a ring around the central peak by stimulated quenching (depletion) using photons of the second wavelength [17,63]. Total internal reflection fluorescence (TIRF) uses a form of structured illumination that excites a thin optical section only 100–300 nm thick adjacent to a refractive index boundary such as a cover glass. This is achieved by shining oblique illumination into the sample. Rays above a critical angle (known as the Brewster angle) for a given wavelength and refractive index difference, do not pass through the interface but are coupled into it, generating a localised 'slice' of illumination called an evanescent wave that falls off exponentially with distance from the boundary in just a few 100 nm. With the proviso that the sample must be closely associated with a suitable refractive index boundary, this is becoming an important method of imaging thin sections of fluorescence particularly in applications looking at cell-substrate and cell surface interactions.

6.6. Computational methods of optical sectioning

Fluorescence microscopy, and LSM techniques in particular, have two qualities that make them especially suitable for computational image processing to improve apparent resolution. Firstly, due to the randomisation of phase during the excited state, fluorescent emissions from different points within the focussed beam do not constructively and destructively interfere like bright-field imaging modes, they just add together to produce the final result. Secondly, the PSF is approximately spatially invariant, i.e. it does not change significantly throughout the image. This is only true if the correct measures have been taken to counter problems associated with mismatch of the refractive index of lens immersion and sample mounting medium, such as spherical aberration. This is a critical factor in the success or failure of restoration methods for LSM data. Adherence to these two criteria enables an image containing contributions from an unknown specimen and a known PSF to be computationally 'deconvolved' to yield a fluorescent distribution closer to that of the underlying specimen [64].

Most image restoration algorithms make use of the fundamental condition that an image can be described as the fluorescence distribution of the object with each point of the object 'replaced' by a representation of the microscope PSF or blurring function. This process is mathematically described as the image (i) equal to a convolution of the object intensity (o) with the PSF (p):

$$i = o \otimes p \tag{5}$$

If the Fourier transform of both sides of this equality are computed the convolution becomes an equality of the transform of i (I) with the product of the transform of o (O) multiplied by the transform of p (P).

$$I = O \times P \tag{6}$$

It might seem that the convolution could be reversed (producing an estimate of O from a measured image) by dividing O by P and Fourier transforming back to the original image. However, this division is very noise-sensitive for regions of the transform close to zero and not defined at all for regions of P that are zero. Some tricks can be employed (such as adding some constant background) to reduce these problems but the results are still unreliable. A better method is to use an iterative estimation procedure to derive the result. This consists in its most basic form of three steps:

(1) Estimating a starting image.
(2) Convolving the image estimate with a measured (or theoretically calculated) PSF.
(3) Comparing the result of (2) with the original image and adjusting the estimate to attempt to correct the difference. Then repeating from (1).

Differences between the various restoration algorithms are centred on the way in which the image 'guess' is updated as well as noise-countering processing such as filtering between each cycle.

In some cases both image and PSF may be restored by a so-called 'blind' algorithm [65] where the PSF is initially 'guessed' (or estimated from known optical parameters). These algorithms have an advantage that they can be extended to allow the PSF to vary throughout the volume, partly accounting for some aberrations. This is conveniently achieved by splitting a 3-D volume up into sub-volumes and allowing the PSF to vary between volumes, each of which is restored independently before being 'melded' together at the end of the computation. This approach can benefit greatly from parallel multi-processor architectures. Ultimately, the s/n in the image and the accuracy of the PSF supplied (or calculated) jointly determine how faithful the restoration is to the true distribution of the specimen.

6.7. Hybrid optical and computational methods

These approaches are based on the notion that the regular microscope response can be improved by a combination of PSF engineering, often by 'structured illumination' followed by a digital image restoration. We might include in this category a range of obvious candidates such as digitally restored confocal images, particularly if a 'sub-optimum' method (e.g. such as using a slit aperture) were employed. More sophisticated methods have recently been devised that produce optical sections from a sequence of wide-field images collected using sequential translation of a grid of structured illumination [66]. A post-processing algorithm is then able to remove the out-of-focus features to leave an optical section that is generally intermediate between a regular image and an optimised confocal result.

6.8. Automated fluorescence imaging: HTS/HCS systems

Automated sample handling and medium-large scale screening are now increasingly important in today's research activities. The flexibility, and thus necessary complexity, of a research microscope is a major impediment to the rapid sampling of many identical specimens. Automation of the standard microscope has helped in this respect but a dedicated instrument is needed if throughput is to be significantly increased and reproducibility maintained. Automated systems are typically designed around a standard range of sample consumables, e.g. 96 or 384 well micro plates. CCD, PMT-based LSM and hybrid systems are all commercially available. Typical automated processes include auto focus, multi-well imaging, repetitive imaging of wells for timed events as well as extensive data handling and bioinformatics. A simple imager is obtained by adding a motorised stage to an inverted microscope. For plastic micro-plates, a lens with variable correction collar is used, compensating for variations in base thickness.

7. Which instrument?—More 'horses for courses'

The advantages of, for example, confocal LSM versus conventional CCD imaging on a fluorescence microscope are self-evident if optical sections are necessary to properly record the results of an experiment. Indeed the starting point for any choice of instrumentation should be consideration of the type of data required, e.g. time-lapse (fast or slow), 3-D/4-D, multi-channel/spectral, high resolution and/or optical sectioning etc, etc. When sectioning is not required, the signal advantages of parallel light collection by sensitive CCDs usually outweigh any of the sophistication of LSMs. One class of application is an exception to this general rule that of localised illumination (e.g. FRAP, FLIP, photo-activation etc). The controlled illumination of LSMs makes them ideal for 'patterned illumination' of (for example) intracellular organelles. The confocal LSM, operated with a large (or no) confocal aperture, provides superior results compared to wide-field illumination through a field-restricting aperture. More localised illumination that is restricted to the focal plane (optical section) is possible with multi-photon excitation.

In many cases imaging information is not actually required. Often, digital images are analysed by measuring total or average intensity of a delineated feature. It is often more efficient to use selected or localised illumination to excite a defined region and to integrate the emitted light from this feature directly on the detector. Many imaging experiments can benefit from a combination of imaging techniques and non-imaging measurement.

Multi-channel imaging (e.g. of multiple fluorescent probes) can be done sequentially (collecting each channel before changing the illumination and filters for the next probe etc) or simultaneously (splitting the light to several detectors, each receiving a defined spectral band). Simultaneous multi-channel imaging is difficult to achieve with high sensitivity single-chip image arrays and colour devices are not usually sensitive enough for low levels of fluorescence and do not allow individual gain control for each probe imaged (necessary when different levels of staining in each channel are encountered). All classes of LSM are especially designed for multi-channel imaging when the de-scanned beam is used for detection. Small filters (or other spectral devices) can be used with the stationary fluorescence beam and splitting the beam to several PMTs is both simple and cost-effective.

When optical sections are required, the choice is between wide-field (conventional) imaging with digital processing, with or without structured illumination techniques. These methods tend to work best when the sample is well understood, and well controlled, and the optical arrangement at the sample can be optimised to reduce the contribution from aberrations. Direct optical sections are often seen as more convenient, although the point-scanning confocal and multi-photon LSM arrangements intrinsically operate with relatively low levels of detected light due to the short pixel times employed. Slit-scanning LSMs, or other arrangements using multiple excitation points, help to bridge the gap towards the sensitivity advantages with CCD detection of wide-field images.

8. Conclusions

Fluorescence-based assays must incorporate many levels of design in order to ensure they accurately reflect a key process of interest in drug delivery research. Central to the assay is the fluorescent probe that consists of two main components (i) the targeting portion and (ii) the chromophore portion, which presents the signal to be measured. The robustness and dynamic range of the assay is dictated by the efficacy of the ligand-target interaction together with the quantum efficiency of the fluorophore. The choice of fluorescent instrument is determined by the nature of the intensity signal to be detected and the required spatiotemporal resolution. Steady-state intensity measurements reflect the amount or concentration of fluorescent probe and the localisation of this signal. Advanced read-out modes (e.g. lifetime, anisotropy, etc.) offer rich information such as the binding of probe with target and the environment in which the probe interacts. The critical challenge in pharmaceutical research is to multiplex the fluorescent assay and package the acquisition and analysis algorithms such that they offer pragmatic solutions for advancing our understanding of drug discovery and delivery.

References

[1] P.C. Cheng, A. Kriete, Image contrast in confocal light microscopy, in: J.B. Pawley (Ed.), The Handbook of Biological Confocal Microscopy, Plenum Press, New York, 1995, pp. 281–310.
[2] F. Zernike, How I discovered phase contrast, Science 121 (1955) 345–349.
[3] K. Schindl, O. Rueker, Differential interference contrast for transmitted-light (Nomarski method), J. Biol. Photogr. Assoc. 41 (1973) 109–111.
[4] R. Hoffman, L. Gross, The modulation contrast microscope, Nature 254 (1975) 586–588.
[5] A.S. Todd, W.K. Barnetson, Use of dark ground microscopy in haematology, J. Clin. Pathol. 41 (1988) 786–792.
[6] J. Bereiter-Hahn, C.H. Fox, B. Thorell, Quantitative reflection contrast microscopy of living cells, J. Cell Biol. 82 (1979) 767–779.
[7] R.P. Haugland, Handbook of Fluorescent Probes and Research Products, 9th ed., Molecular Probes, 2000.
[8] P. Warson, A.T. Jones, D.J. Stephens, Intracellular trafficking pathways and drug delivery: Fluorescence imaging of living and fixed cells, Adv. Drug Deliv. Rev. 57 (2005) 43–61. This Issue.
[9] R. Stevenson, Biosensors: surface plasmon resonance lights the way, Am. Biotechnol. Lab. 9 (1991) 36.
[10] L.G. Fagerstam, A. Frostell, R. Karlsson, M. Kullman, A. Larsson, M. Malmqvist, H. Butt, Detection of antigen–antibody interactions by surface plasmon resonance, Application to epitope mapping, J. Mol. Recognit. 3 (1990) 208–214.
[11] D.C. Cullen, R.G. Brown, C.R. Lowe, Detection of immunocomplex formation via surface plasmon resonance on gold-coated diffraction gratings, Biosensors 3 (1987) 211–225.
[12] D.B. Shear, The generalized Boltzmann distribution, J. Theor. Biol. 39 (1973) 165–169.
[13] M. Born, E. Wolf, Principles of Optics, 5th ed., Pergamon, New York, 1975.
[14] M. Goppert-Meyer, Ueber elementerakte mit zwei Quantenspruengen, Ann. Phys. (Leipz.) 9 (1931) 273–295.
[15] W. Denk, J.H. Strickler, W.W. Webb, Two-photon laser scanning fluorescence microscopy, Science 248 (1990) 73–76.

[16] N. Ben-Tuvim, Laser-light amplification by stimulated emission of radiation, Harefuah 65 (1963) 191–194.
[17] M. Dyba, S.W. Hell, Photostability of a fluorescent marker under pulsed excited-state depletion through stimulated emission, Appl. Opt. 42 (2003) 5123–5129.
[18] T.A. Klar, S. Jakobs, M. Dyba, A. Egner, S.W. Hell, Fluorescence microscopy with diffraction resolution barrier broken by stimulated emission, Proc. Natl. Acad. Sci. U. S. A. 97 (2000) 8206–8210.
[19] D.E. Koppel, D. Axelrod, J. Schlessinger, E.L. Elson, W.W. Webb, Dynamics of fluorescence marker concentration as a probe of mobility, Biophys. J. 16 (1976) 1315–1329.
[20] A.E. McGrath, C.G. Morgan, G.K. Radda, Photobleaching. A novel fluorescence method for diffusion studies in lipid system, Biochim. Biophys. Acta 426 (1976) 173–185.
[21] V. Chen, Non laser light sources, in: J.B. Pawley (Ed.), The Handbook of Biological Confocal Microscopy, Plenum Press, New York, 1995, pp. 99–109.
[22] E. Gratton, M.J. van de Ven, Laser sources for confocal microscopy, in: J.B. Pawley (Ed.), The Handbook of Biological Confocal Microscopy, Plenum Press, New York, 1995, pp. 69–97.
[23] J.B. Pawley, Fundamental limits in confocal microscopy, in: J.B. Pawley (Ed.), The Handbook of Biological Confocal Microscopy, Plenum Press, New York, 1995, pp. 19–37.
[24] D.R. Sandison, R.M. Williams, K.S. Wells, J. Strickler, W. Webb, Quantitative fluorescence confocal laser scanning microscopy, in: J.B. Pawley (Ed.), The Handbook of Biological Confocal Microscopy, Plenum Press, New York, 1995, pp. 39–53.
[25] J. Art, Photon detectors for confocal microscopy, in: J.B. Pawley (Ed.), The Handbook of Biological Confocal Microscopy, Plenum Press, New York, 1995, pp. 183–196.
[26] T. Zimmermann, J. Rietdorf, R. Pepperkok, Spectral imaging and its applications in live cell microscopy, FEBS Lett. 546 (2003) 87–92.
[27] J.R. Lackowicz, Time-resolved laser spectroscopy in biochemistry, Proc. SPIE 909 (1988) 23–28.
[28] E. Gratton, D.M. Jameson, R.D. Hall, Multifrequency phase and modulation fluorometry, Annu. Rev. Biophys. Bioeng. 13 (1984) 105–124.
[29] X.F. Wang, S. Kitayama, T. Uchida, D.M. Coleman, S. Minami, A two-dimensional fluorescence lifetime imaging system using a gated image intensifier, Appl. Spectrosc. 45 (1991) 360–366.
[30] X.F. Wang, S. Kitayama, T. Uchida, D.M. Coleman, S. Minami, Time-resolved fluorescence microscopy using multichannel photon counting, Appl. Spectrosc. 44 (1990) 25–30.
[31] G. Weber, Rotational Brownian motion and polarization of the fluorescence of solutions, Adv. Protein Chem. 8 (1953) 415–459.
[32] G. Weber, Polarization of the fluorescence of macromolecules. I. Theory and experimental method, Biochem. J. 51 (1952) 145–155.
[33] P. Johnson, E.G. Richards, A simple instrument for studying the polarization of fluorescence, Arch. Biochem. Biophys. 97 (1962) 250–259.
[34] K. Jacobson, Z. Derzko, E.S. Wu, Y. Hou, G. Poste, Measurement of the lateral mobility of cell surface components in single, living cells by fluorescence recovery after photobleaching, J. Supramol. Struct. 5 (1976) 565–576.
[35] J. White, E.H. Stelzer, Photobleaching GFP reveals protein dynamics inside live cells, Trends Cell Biol. 9 (1999) 61–65.
[36] J. Lippincott-Schwartz, N. Altan-Bonnet, G.H. Patterson, Photobleaching and photoactivation: following protein dynamics in living cells, Nat. Cell Biol. Suppl. (2003) S7–S14.
[37] S.C. De Smedt, K. Remaut, B. Lucas, K. Braeckmans, N.N. Sanders, J. Demeester, Studying biophysical barriers to DNA delivery by advanced light microscopy, Adv. Drug Deliv. Rev. 57 (2005) 191–210. This Issue.
[38] K.E. Sawin, P. Nurse, Photoactivation of green fluorescent protein, Curr. Biol. 7 (1997) R606–R607.
[39] A. Ishihara, K. Gee, S. Schwartz, K. Jacobson, J. Lee, Photoactivation of caged compounds in single living cells: an application to the study of cell locomotion, BioTechniques 23 (1997) 268–274.
[40] G.H. Patterson, J. Lippincott-Schwartz, A photoactivatable GFP for selective photolabeling of proteins and cells, Science 297 (2002) 1873–1877.
[41] A. Pramanik, R. Rigler, Ligand-receptor interactions in the membrane of cultured cells monitored by fluorescence correlation spectroscopy, Biol. Chem. 382 (2001) 371–378.
[42] Y. Nomura, H. Tanaka, L. Poellinger, F. Higashino, M. Kinjo M, Monitoring of in vitro and in vivo translation of green fluorescent protein and its fusion proteins by fluorescence correlation spectroscopy, Cytometry 44 (2001) 1–6.
[43] M. Gösch, R. Rigler, Fluorescence correlation spectroscopy of molecular motions and kinetics, Adv. Drug Deliv. Rev. 57 (2005) 169–190. This Issue.
[44] M.R. Melamed, Z. Darzynkiewicz, F. Traganos, T. Sharpless, Cytology automation by flow cytometry, Cancer Res. 37 (1977) 2806–2812.
[45] J.S. Ploem, A study of filters and light sources in immunofluorescence microscopy, Ann. N.Y. Acad. Sci. 177 (1971) 414–429.
[46] J.S. Ploem, A new microscopic method for the visualization of blue formaldehyde-induced catecholamine fluorescence, Arch. Int. Pharmacodyn. Ther. 182 (1969) 421–424.
[47] J.S. Ploem, The use of a vertical illuminator with interchangeable dichroic mirrors for fluorescence microscopy with incidental light, Z. Wiss. Mikrosk. 68 (1967) 129–142.
[48] C.W. McCutchen, Superresolution in microscopy and the Abbe resolution limit, J. Opt. Soc. Am. 57 (1967) 1190–1192.
[49] D.M. Maurice, A scanning slit optical microscope, Invest. Ophthalmol. 13 (1974) 1033–1037.
[50] T. Wilson, C.J.R. Sheppard, Scanning Optical Microscopy, Academic Press, San Diego, 1984.
[51] M. Petran, M. Hadravsky, M.D. Egger, R. Galambos, Tandem scanning reflected light microscope, J. Opt. Soc. Am. 58 (1968) 661–664.
[52] T. Tanaami, S. Otsuki, N. Tomosada, Y. Kosugi, M. Shimizu, H. Ishida, High-speed 1-frame/ms scanning confocal microscope with a microlens and Nipkow disks, Appl. Opt. 41 (2002) 4704–4708.

[53] I.J. Cox, Scanning optical fluorescence microscopy, J. Microsc. 133 (1984) 149–154.
[54] E.H.K. Stelzer, The intermediate optical system of laser scanning confocal microscopes, in: J.B. Pawley (Ed.), The Handbook of Biological Confocal Microscopy, Plenum Press, New York, 1995, pp. 139–153.
[55] A. Draiijer, P.M. Houpt, A standard video-rate confocal laser-scanning refection and fluorescence microscope, Scanning 10 (1988) 139–145.
[56] G.J. Brakenhoff, H.T. van der Voort, E.A. van Spronsen, N. Nanninga, Three-dimensional Imaging of biological structures by high resolution confocal scanning laser microscopy, Scanning Microsc. 2 (1988) 33–40.
[57] J.G. White, W.B. Amos, M. Fordham, An evaluation of confocal versus conventional imaging of biological structures by fluorescence light microscopy, J. Cell Biol. 105 (1987) 41–48.
[58] C.J. Sheppard, T. Wilson, The theory of the direct-view confocal microscope, J. Microsc. 124 (1981) 107–117.
[59] R.J. Errington, S.M. Ameer-beg, B. Vojnovic, L.H. Patterson, M. Zloh, P.J. Smith, Advanced microscopy solutions for monitoring the kinetics and dynamics of drug-DNA targeting in living cells, Adv. Drug Deliv. Rev. 57 (2005) 153–167. This Issue.
[60] G.M. Tozer, S.M. Ameer-beg, J. Baker, P.R. Barber, S.A. Hill, R.J. Hodgkiss, R. Locke, V.E. Prise, I. Wilson, B. Vojnovic, Intravital imaging of tumour vascular networks using multi-photon fluorescence microscopy, Adv. Drug Deliv. Rev. 57 (2005) 135–152. This Issue.
[61] T.D. Wang, M.J. Mandella, C.H. Contag, G.S. Kino, Dual-axis confocal microscope for high-resolution in vivo imaging, Opt. Lett. 28 (2003) 414–416.
[62] M. Schrader, K. Bahlmann, G. Giese, S.W. Hell, 4Pi-confocal imaging in fixed biological specimens, Biophys. J. 75 (1998) 1659–1668.
[63] S.W. Hell, Toward fluorescence nanoscopy, Nat. Biotechnol. 21 (2003) 1347–1355.
[64] J.R. Swedlow, Quantitative fluorescence microscopy and image deconvolution, Methods Cell Biol. 72 (2003) 349–367.
[65] T.J. Holmes, Blind deconvolution of quantum-limited incoherent imagery: maximum-likelihood approach, J. Opt. Soc. Am. 9 (1992) 1052–1061.
[66] M.A.A. Neil, R. Juskaitis, T. Wilson, Method of obtaining optical sectioning by using structured light in a conventional microscope, Opt. Lett. 22 (2003) 1905–1907.
[67] A. Mobasheri, R.J. Errington, S. Golding, A.C. Hall, J.P. Urban, Characterization of the Na+, K+-ATPase in isolated bovine articular chondrocytes; molecular evidence for multiple alpha and beta isoforms, Cell Biol. Int. 21 (1997) 201–212.
[68] A. Watson, X. Wu, M. Bruchez, Lighting up cells with quantum dots, BioTechniques 34 (2003) 296–300.
[69] M.E. Akerman, W.C. Chan, P. Laakkonen, S.N. Bhatia, E. Ruoslahti, Nanocrystal targeting in vivo, Proc. Natl. Acad. Sci. U. S. A. 99 (2002) 12617–12621.
[70] M.S. Kayne, M. Cohn, Enhancement of Tb(III) and Eu(III) fluorescence in complexes with Escherichia coli tRNA, Biochemistry 13 (1974) 4159–4165.
[71] J.M. Wolfson, D.R. Kearns, Europium as a fluorescent probe of metal binding sites on transfer ribonucleic acid: I. Binding to Escherichia coli formylmethionine transfer ribonucleic acid, J. Am. Chem. Soc. 96 (1974) 3653–3654.
[72] C. Formoso, Fluorescence of nucleic acid-terbium (3) complexes, Biochem. Biophys. Res. Commun. 53 (1973) 1084–1087.
[73] R.Y. Tsien, The green fluorescent protein, Annu. Rev. Biochem. 67 (1998) 509–544.
[74] R. Rizzuto, M. Brini, F. De Giorgi, R. Rossi, R. Heim, R.Y. Tsien, T. Pozzan, Double labelling of subcellular structures with organelle-targeted GFP mutants in vivo, Curr. Biol. 6 (1996) 183–188.
[75] R. Heim, D.C. Prasher, R.Y. Tsien, Wavelength mutations and posttranslational autoxidation of green fluorescent protein, Proc. Natl. Acad. Sci. U. S. A. 91 (1994) 12501–12504.
[76] R. Heim, R.Y. Tsien, Engineering green fluorescent protein for improved brightness, longer wavelengths and fluorescence resonance energy transfer, Curr. Biol. 6 (1996) 178–182.
[77] R.Y. Tsien, A. Miyawaki, Seeing the machinery of live cells, Science 280 (1998) 1954–1955.
[78] L.A. Gross, G.S. Baird, R.C. Hoffman, K.K. Baldridge, R.Y. Tsien, The structure of the chromophore within DsRed, a red fluorescent protein from coral, Proc. Natl. Acad. Sci. U. S. A. 97 (2000) 11990–11995.
[79] B.A. Griffin, S.R. Adams, J. Jones, R.Y. Tsien, Fluorescent labelling of recombinant proteins in living cells with FlAsH, Methods Enzymol. 327 (2000) 565–578.